Published in final edited form as:

Cancer Res. 2021 May 01; 81(9): 2275–2288. doi:10.1158/0008-5472.CAN-20-1541.

Exogenous and endogenous sources of serine contribute to colon cancer metabolism, growth, and resistance to 5-fluorouracil

David C. Montrose[1,2], **Suchandrima Saha**[1], **Miguel Foronda**[3], **Erin M. McNally**[3], **Justin Chen**[3], **Xi Kathy Zhou**[4,9], **Taehoon Ha**[4], **Jan Krumsiek**[5,9,10], **Mustafa Buyukozkan**[5], **Akanksha Verma**[5], **Olivier Elemento**[5,9,10], **Rhonda K. Yantiss**[6], **Qiuying Chen**[7], **Steven S. Gross**[7,9], **Lorenzo Galluzzi**[8,9,10,11,12], **Lukas E. Dow**[3,9], **Andrew J. Dannenberg**[3,9]

[1]Department of Pathology, Renaissance School of Medicine, Stony Brook University, Stony Brook, NY, USA;

[2]Stony Brook Cancer Center, Stony Brook, NY, USA;

[3]Departments of Medicine, Weill Cornell Medical College, New York, NY, USA;

[4]Departments of Healthcare Policy and Research, Weill Cornell Medical College, New York, NY, USA;

[5]Departments of Physiology and Biophysics, Weill Cornell Medical College, New York, NY, USA;

[6]Departments of Pathology and Laboratory Medicine, Weill Cornell Medical College, New York, NY, USA;

[7]Departments of Pharmacology, Weill Cornell Medical College, New York, NY, USA;

[8]Departments of Radiation Oncology, Weill Cornell Medical College, New York, NY, USA;

[9]Sandra and Edward Meyer Cancer Center, New York, NY, USA;

[10]Caryl and Israel Englander Institute for Precision Medicine, New York, NY, USA;

[11]Department of Dermatology, Yale School of Medicine, New Haven, CT, USA;

[12]Université de Paris, Paris, France.

Abstract

Serine is a non-essential amino acid generated by the sequential actions of phosphoglycerate dehydrogenase (PHGDH), phosphoserine aminotransferase (PSAT1), and phosphoserine phosphatase (PSPH). Increased serine biosynthesis occurs in several cancers and supports tumor

Corresponding Author: David C. Montrose, Department of Pathology, Renaissance School of Medicine, Stony Brook University, MART Building, 9M-0816, Lauterbur Dr., Stony Brook, NY 11794. Phone: 631-216-2927; Fax: 631-444-3424; david.montrose@stonybrookmedicine.edu.

Authors' Contributions

D.C.M., M.F., S.S., E.M., J.C. and Q.C. performed experiments. X.K.Z., T.H., J.K., A.V., O.E. M.B. and Q.C. carried out data analysis. R.K.Y. provided patient samples and sample analysis. D.C.M., S.S.G., Q.C., J.K., L.G., L.E.D. and A.J.D. designed experiments and interpreted data. D.C.M., J.K., L.G. and A.J.D. contributed to manuscript preparation.

Declaration of interests: L.G. received consulting fees from OmniSEQ, Astra Zeneca, Inzen and the Luke Heller TECPR2 Foundation, and is a member of the Scientific Advisory Committee of Boehringer Ingelheim, The Longevity Labs and OmniSEQ.

growth. Additionally, cancer cells can harness exogenous serine to enhance their metabolism and proliferation. Here we tested the relative contributions of exogenous and endogenous sources of serine on the biology of colorectal cancer (CRC). In murine tumors, Apc status was identified as a determinant of the expression of genes controlling serine synthesis. In patient samples, PSAT1 was overexpressed in both colorectal adenomas and adenocarcinomas. Combining genetic deletion of PSAT1 with exogenous serine deprivation maximally suppressed the proliferation of CRC cells and induced profound metabolic defects including diminished nucleotide production. Inhibition of serine synthesis enhanced the transcriptional changes following exogenous serine removal as well as alterations associated with DNA damage. Both loss of PSAT1 and removal of serine from the diet were necessary to suppress CRC xenograft growth and enhance the anti-tumor activity of 5-fluorouracil (5-FU). Restricting endogenous and exogenous serine *in vitro* augmented 5-FU induced cell death, DNA damage, and metabolic perturbations, likely accounting for the observed anti-tumor effect. Collectively, our results suggest that both endogenous and exogenous sources of serine contribute to CRC growth and resistance to 5-FU.

Keywords

diet; chemotherapy; DNA damage

Introduction

Serine is a non-essential amino acid that can be generated from the glucose intermediate 3-phosphoglycerate by the sequential actions of phosphoglycerate dehydrogenase (PHGDH), phosphoserine aminotransferase (PSAT1) and phosphoserine phosphatase (PSPH). Serine biosynthesis is increased in several cancers and supports tumor growth (1–9). This growth-promoting effect of serine occurs primarily as a consequence of enhanced one-carbon metabolism (1–3,10). For example, serine is a major donor of one-carbon units that are utilized to stimulate nucleotide synthesis, glutathione production and methylation, among other effects (1–3,10). Importantly, exogenous serine can also be taken up by cancer cells to fuel tumor growth (1–3). In fact, previous work has shown that removal of either exogenous serine in culture or the combination of serine and glycine in diet can suppress colorectal cancer (CRC) cell proliferation and xenograft/intestinal tumor growth, respectively (11,12). Additionally, exogenous serine deprivation results in considerable adaptations of cellular metabolism (11,13). Interestingly, colon cancer cells upregulate serine biosynthesis enzymes in response to deprivation of exogenous serine, suggesting a compensatory adaptive response to reduced availability of serine (11). In fact, impairing the ability of cancer cells to synthesize serine renders them more susceptible to the anti-proliferative effects of serine-deprivation *in vitro* and *in vivo* (14,15). Moreover, cancer cells and tumors with high expression of PHGDH have a growth advantage over their low PHGDH-expressing counterparts when grown in a low serine environment (16,17).

Studies using lymphoma and hepatocellular carcinoma cells have suggested that genes encoding serine synthesis enzymes are induced in response to activation of Wnt signaling (18–20). Mutation of the *APC* gene occurs in approximately 80% of sporadic colorectal tumors and activates Wnt signaling, leading to enhanced expression of numerous pro-

proliferative genes (21). Given the significance of increased Wnt signaling in the pathogenesis of CRC, and the role of this pathway in regulating the expression of serine synthesis genes, it is likely that enhanced serine synthesis supports the development and progression of colorectal tumors. In support of this concept, elevated serine levels were found in murine colon tumors and human CRC (22,23). Furthermore, elevated *PSAT1* expression was observed in CRC and accompanying hepatic metastases; and overexpression of PSAT1 in CRC cells enhanced xenograft growth (8).

Despite evidence that both endogenous and exogenous sources of serine can support tumor growth and data suggesting an interplay between these sources, their relative contributions to the biology of CRC is unclear. The current study was carried out to determine the roles of exogenous and endogenous serine sources in supporting the growth of CRC and whether reducing serine availability impacts the efficacy of chemotherapy. Here we show that activation of Wnt signaling leads to increased expression of genes controlling serine synthesis in murine intestinal tumors. Notably, elevated levels of PSAT1 were observed in early and advanced colonic neoplasia in humans. Limiting both endogenous and exogenous sources of serine maximally suppressed CRC cell proliferation, altered metabolism and enhanced susceptibility to 5-fluorouracil (5-FU)-induced cell death, resulting in anti-neoplastic effects *in vivo*. Taken together, our results suggest that the combination of inhibiting serine synthesis and reducing its availability from exogenous sources may limit CRC growth and enhance the anti-tumor activity of 5-FU.

Materials and Methods

Mouse studies

Male $Apc^{Min/+}$ and wild-type (WT) mice from the same colony were obtained from The Jackson Laboratory at 4 weeks of age and placed on AIN-93G purified diet (Research Diets).

All mice were sacrificed at 16 weeks of age at which time the distal small intestine was harvested and flushed with ice cold phosphate buffered saline. Intestine was cut open longitudinally and polyps were collected from $Apc^{Min/+}$ mice and normal ileal mucosa was collected from WT mice by scraping with a glass slide. Tissues were snap-frozen and stored at −80°C until the analysis of gene expression.

For xenograft studies of tumor growth, 40 male athymic nude mice were obtained from the Jackson Laboratory at 6 weeks of age. Half of the mice were injected subcutaneously with 0.5 million empty vector (EV) or PSAT1KO HCT116 cells suspended in a mixture of matrigel and serum-free DMEM in a 1:1 ratio in both flanks; the remaining mice were injected subcutaneously in both flanks with 0.5 million EV or PSAT1KO DLD1 cells suspended in a mixture of matrigel and serum-free DMEM in a 1:1 ratio. Two days later, half of the mice were placed on AIN-93G-based complete amino acid based diet or the same diet lacking serine (Research Diets) (Supplementary Table S1). Tumor volume was measured weekly using calipers.

For xenograft studies testing the effects of 5-FU, 60 male athymic nude mice were obtained from the Jackson Laboratory at 6 weeks of age. Half of the mice were injected subcutaneously in the flank with 1 million EV HCT116 cells and the remaining mice were injected with PSAT1KO HCT116 cells; all cells were suspended in a mixture of matrigel and serum-free DMEM in a 1:1 ratio. Mice were maintained on AIN-93G diet and tumors were allowed to grow for 20 days until they reached a palpable size (~300mm^2). Mice injected with EV cells were then given complete (Comp) diet and divided into two groups that received either 75mg/kg 5-FU dissolved in 0.9% saline or vehicle, *via* intraperitoneal injections every 3–4 days over 11 days. At the same time, mice inoculated with PSAT1KO cells were given serine deficient (Ser Def) diet and either 5-FU or vehicle. Tumor volume was measured using calipers. All mice were housed under specific pathogen free conditions in rooms maintained at 70°F. All animal studies were approved by the Institutional Animal Care and Use Committee (IACUC) at Weill Cornell Medicine (WCM).

Generation of PSAT1KO cells

Cells were purchased from American Type Culture Collection and used within 10 passages for all experiments. Cells were confirmed to be mycoplasma free periodically during the course of the study using the MycoProbe mycoplasma detection kit (R&D Systems). To generate PSAT1KO cells, DLD1, HCT116 and HEK293T cells were cultured in Dulbecco's Modified Eagle's Medium (DMEM) containing 10% FBS and 1% Pen-Strep. To prepare viral supernatants, 2.5×10^5 HEK293T cells were plated onto 35mm wells and transfected with 5μg DNA backbone + 1.25μg PAX2 and 1.25μg VSVG packaging vectors using 30μl PEI in 100μl DMEM. Lentiviral supernatants were collected at 36, 48 and 72 hours, pooled and cleared by centrifugation (10 minutes at 2000rpm) and stored at −80°C until use. 5–10×10^4 target cells were seeded onto 24 well plates and 24 hours later were transduced using serial dilutions of the lentiviral supernatants containing 8μg/ml Polybrene. Cells were selected or assessed by flow cytometry 48 hours post-transduction. To generate Cas9-expressing DLD1 and HCT116 clones, cells were transduced with pLenti-Cas9-P2A-Puro, selected for 2 days in 2μg/ml Puromycin and cells were plated in limiting dilution in 96 well plates as previously described (24). After 5–10 days, single cell-derived clones were picked, expanded and functionally selected based on their response to RPA and CDK1 gRNAs. At least three independent clones were used for functional tests. Guide RNAs (gRNAs) were transduced using the pLenti-U6gRNA-EF1-tdTomato-P2A-Blasticidin (*LRT2B*) vector which was produced through Gibson assembly by replacing GFP from a pLenti-U6-gRNA-EF1-GFP (LRG) backbone (24). Sequences of gRNAs are shown in Supplementary Table S2. Assessment of Cas9-induced mutagenesis was carried out by T7 assays as previously described (25). Briefly, target loci in PSAT1 gene for each of the gRNA constructs were PCR amplified from LRT2B-transduced and Blasticidin-selected cells (10μg/ml for 5 days) using Herculase II Fusion polymerase (Agilent) according to the following program: 98˚C x 3:00, 98˚C - 0:45 → 58˚C - 0:45 → 72˚C - 1:00 × 34 cycles, 72 ˚C x 3:00. Primers used were PS1-gR1-T7-F and PS1-gR1-T7-R, PS1-gR2-T7-F and PS1-gR2-T7-R and PS1-gR4-T7-F and PS1-gR4-T7-R (For gRNA sites 1, 2 and 4, respectively). All the primers are listed in Supplementary Table S3.

Cell-based assays

Cell proliferation was assessed by estimating the cell count based on CountBright™ absolute counting beads (ThermoFisher). Briefly, 2×10^4 EV or PSAT1 KO HCT116 or 8×10^4 EV or PSAT1 KO DLD1 cells were seeded into 6-well plates and serum starved for 18 hr. Cells were then washed and incubated in complete or serine deficient media and/or formate for the indicated number of days. On the day of analysis, cells were harvested, stained with 4',6-diamidino-2-phenylindole (DAPI) (Sigma-Aldrich) and 50 μl of counting beads were added. The samples were acquired by BD LSRFortressa II flow cytometer with 488-nm excitation at the Flow Cytometry Core Facility of Stony Brook University. Cell concentration was calculated using the formula provided by the manufacturer and relative cell number on each day was determined by comparing to day 0.

To determine cell viability, 1×10^4 EV or PSAT1 KO cells were seeded on 6-well plates and treated as indicated. Cells were then harvested and stained for 30 minutes at 37°C with 20 nmol/L of 3,3'-Dihexyloxacarbocyanine iodide (DiOC6(3)) (Sigma-Aldrich) followed by staining with 1 μg/mL DAPI for 5 minutes, and subjected to flow cytometric analysis using a BD LSRFortressa II flow cytometer with 405 and 488-nm excitation. DIOC6(3) positive and DAPI negative cells were considered live.

Complete medium was made based on Minimal Essential Medium (MEM) (Gibco) (which does not contain serine or glycine) supplemented with 10% dialyzed fetal bovine serum (Gibco), MEM vitamin mix, 1% pen/strep, D-glucose (4.5g/L), glycine (0.4mmol/L) and serine (0.4mmol/L). Serine deficient medium contained the same components as complete medium except for serine.

For detection of 53BP1, cells were seeded onto coverslips at a density of 200,000 cells per well in 2ml of media in 6 well plates. Following complete or serine deficient media and/or formate treatment, coverslips were washed with phosphate buffered saline (PBS), fixed in PBS containing 4% paraformaldehyde for 15 min at room temperature, washed with PBS and subjected to permeabilization in PBS supplemented with 0.1% Triton X-100. Cells were then washed three times with PBS and incubated for 1 hr at room temperature in blocking buffer (PBS containing 2% BSA). Cells were then incubated overnight with rabbit anti-53BP1 (NB100–304; Novus Biologicals Ltd; 1:500) primary antibody diluted in blocking buffer. Cells were washed three times in PBS and incubated with goat anti-rabbit Alexa Fluor 647 (A21244; ThermoFisher; 1:3000) secondary antibody diluted in blocking buffer for 1 hr at room temperature. Cells were further washed with PBS then mounted with DAPI Fluoromount-G (0100–20; SouthernBiotech). The images were captured using a 405 nm laser (DAPI) and white light laser (53BP1) using a 63X objective then magnified 2X using a Leica TCS SP8 X confocal microscope. 53BP1 was quantified by first determining the average number of positive foci per cell in the control group. The percent of cells with a number of foci greater than the average of the controls was then determined in all groups and reported. Counting was based on quantifying 4 fields per sample in 3 replicates with 263–653 total cells counted across each condition/cell line.

RNA-sequencing

EV HCT116 cells were given complete or serine deficient media and PSAT1KO cells were given serine deficient medium for 24 hours then total RNA was isolated using the RNeasy mini kit (Qiagen, Hilden, Germany). Following RNA isolation, total RNA integrity was checked using a 2100 Bioanalyzer (Agilent Technologies, Santa Clara, CA). RNA concentrations were measured using the NanoDrop system (Thermo Fisher Scientific, Inc., Waltham, MA). Preparation of RNA sample library and RNA-seq were performed by the Genomics Core Laboratory at Weill Cornell Medicine. Messenger RNA was prepared using TruSeq Stranded mRNA Sample Library Preparation kit (Illumina, San Diego, CA), according to the manufacturer's instructions and was sequenced on an Illumina HiSeq4000 sequencer with pair-end 50 bp cycles. Sequencing quality was assessed using FastQC (Babraham Bioinformatics, Cambridge, UK). Raw sequenced reads were aligned to the human reference genome (Version mm10 from UCSC) using STAR (Version 2.4.2) aligner. Aligned reads were quantified against the reference annotation (mm10 from UCSC) to obtain Fragments per Kilobase per million (FPKM) and raw counts using *CuffLinks* (v 2.2.1) and *HTSeq*, respectively.

In order to classify the samples based on gene expression profiles, unsupervised hierarchical clustering was performed on log2 transformed FPKM Expression. A total of 23,674, genes were measured. Among them 12,556 had counts per million (CPM) values >1 in at least 2 samples and were kept for differential expression analysis. The differential gene expression analysis used the limma/voom pipeline with counts data normalized using DGEList function from *EdgeR*. For comparison of any 2 given independent groups, genes with FDR < 0.05 and logFC ≥ 1 were considered to be significantly differentially expressed. RNA-seq data were deposited onto GEO and given the GSE144506. The entire dataset can be found at: https://www.ncbi.nlm.nih.gov/geo/query/acc.cgi?acc=GSE144506. All statistical analyses were carried out in R statistical software. Gene name-based pathway analysis was carried out on the RNA-seq results by gene set enrichment analysis using KEGG pathways. A pathway with a FDR < 0.1 was considered to be significantly enriched.

Metabolite profiling

Metabolite profiling of DLD1 and HCT116 EV or PSAT1 KO cells grown in complete or serine deficient media was carried out in the Weill Cornell Medicine Proteomics and Metabolomics Core Facility. Metabolites were extracted by adding pre-cooled 80% methanol, vigorously vortexed and centrifuged at 12,000 x g for 20 minutes at 4 °C. The supernatants were dried by vacuum centrifugation and resuspended in mobile phase. Targeted LC/MS analyses were performed on a Q Exactive Orbitrap mass spectrometer (Thermo Scientific) coupled to a Vanquish UPLC system (Thermo Scientific). The Q Exactive operated in polarity-switching mode. A Sequant ZIC-HILIC column (2.1 mm i.d. × 150 mm, Merck) was used for separation of metabolites. Flow rate was set at 150 μL/min. Buffers consisted of 100% acetonitrile for mobile A, and 0.1% NH_4OH/20 mmol/L CH_3COONH_4 in water for mobile B. Gradient ran from 85% to 30% A in 20 minutes followed by a wash with 30% A and re-equilibration at 85% A. Metabolites were identified on the basis of exact mass within 5 ppm and standard retention times. Relative metabolite quantitation was performed based on peak area for each metabolite. All data analysis was

done using in-house written scripts and metabolite abundance was normalized to cell number.

Prior to statistical analysis, raw metabolite intensities were normalized *via* probabilistic quotient normalization (26) and then $\log_2$-scaled. For differential analysis, all metabolite concentrations were normalized to the EV Comp group, by subtracting the respective metabolite mean of EV Comp from all concentrations (note that subtraction at log scale is equivalent to division). Statistical differences were assessed using two-sample t-tests between EV Comp and the other three groups. Multiple hypothesis testing was corrected by controlling the FDR at 0.1 using the Benjamini-Hochberg procedure (27). Pathway analysis was performed as previously described (28) by first scaling all metabolite concentrations (mean 0, standard deviation 1) and then calculating the average concentration of all metabolites per pathway as a new representative value. This value was then subjected to the same t-tests as above.

Stable isotope tracing

Metabolite tracing was carried out by LC-MS analysis as described previously (29) using a platform comprised of an Agilent Model 1290 Infinity II liquid chromatography system coupled to an Agilent 6550 iFunnel time-of-flight MS analyzer. Chromatography of metabolites utilized aqueous normal phase (ANP) chromatography on a Diamond Hydride column (Microsolv). Mobile phases consisted of: (A) 50% isopropanol, containing 0.025% acetic acid, and (B) 90% acetonitrile containing 5 mmol/L ammonium acetate. To eliminate the interference of metal ions on chromatographic peak integrity and electrospray ionization, EDTA was added to the mobile phase at a final concentration of 6 μmol/L. The following gradient was applied: 0–1.0 minutes, 99% B; 1.0–15.0 minutes, to 20% B; 15.0 to 29.0, 0% B; 29.1 to 37 minutes, 99% B. To determine the fate of hypoxanthine, EV and PSAT1KO cells were cultured in complete or serine deficient media for 12 hours. An in-house untargeted stable isotope tracing (USIT) strategy was carried out to obtain all possible fates of [2,8,9-D3]-hypoxanthine and quantitative information on the relative incorporation of hypoxanthine–derived metabolites based on the stable isotope labeling pattern. Metabolite profiling softwares MassHunter Qualitative Analysis 7.0, MassProfinder 8.0 and MPP 14.9.1 (Agilent) were used to generate a list of differentially-expressed metabolites in cells grown in [2,8,9-D3]- hypoxanthine *vs.* [2,8,9-H3] hypoxanthine or $^{13}C_3$ serine-supplemented media. Differential ion features then served as targets for generating curated isotopologues that are expected to contain incorporated stable isotope elements. To enhance true positive discovery rate and diminish false positives/negatives, the presence of a reciprocal shift in isotopologue spectral patterns, i.e., that incorporation of the heavy isotope occurs concomitantly with a decrease in light isotope content, was confirmed. USIT also calculates and corrects for the natural abundance of heavy isotope in samples. We predict a maximum of 100% steady state enrichment of [2,8,9-D3] hypoxanthine .

Quantitative real-time PCR

Total RNA was isolated from frozen polyps or normal intestinal mucosa using the RNeasy mini kit (Qiagen). RNA was reverse transcribed to make cDNA using murine leukemia virus reverse transcriptase and oligo (dT) 16 primer. The resulting cDNA was used for

amplification using QuantiTect Primer Assays (Qiagen) for the following genes: *Phosphoglycerate dehydrogenase* (*Phgdh*; Mm_Phgdh_2_SG); *Phosphoserine aminotransferase* (*Psat1*; Mm_Psat1_2_SG); *Phosphoserine phosphatase* (*Psph*; Mm_PSPH_1_SG); *Glyceraldehyde 3 phosphate dehydrogenase* (*Gapdh*) was used as an endogenous normalization control (Mm_Gapdh_3_SG). Quantitative real-time PCR was conducted using 2X SYBR green PCR master mix on a 7500 real-time PCR system (Applied Biosystems). Relative fold induction was determined using the ddCT (relative quantification) analysis protocol.

Western blotting

Specimens from patients with colorectal adenocarcinoma were procured at the time of surgery. Tissue samples collected under a protocol approved by the Institutional Review Board at WCM were obtained from resected colon specimens within 15 minutes of their removal. A portion of tumor and a sample of adjacent normal colonic mucosa at a minimum distance of 5 cm from the tumor were harvested by sharp dissection. Samples were immediately stored at −80°C until protein extraction. Tumor and cell lysates were obtained using RIPA Buffer (Sigma Aldrich, St. Louis, MO) containing protease inhibitor and phosphatase inhibitor tablets (Roche Diagnostics, Mannheim, Germany). Protein concentration was determined using the Lowry short method. Proteins were separated by SDS-PAGE and subsequently electro-transferred to nitrocellulose membrane. The membranes were blotted with antibodies towards PSAT1 (Novus, NBP1–32920), PHGDH (Sigma-Aldrich, SAB2101795), PSPH (ThermoFisher, PA5–19113), Phospho-Histone H2AX (Cell Signaling, #2577L) and β-actin (Sigma Aldrich, A3854). Secondary antibodies were then applied. ECL chemiluminescence was utilized to detect the protein bands.

Immunohistochemistry

Sections containing adenoma or adenocarcinoma and adjacent normal tissue were obtained from archival specimens in the WCM Department of Pathology. Paraffin-embedded tissue sections were deparaffinized and incubated with 1% hydrogen peroxide for 20 minutes at room temperature. Sections were subjected to antigen retrieval by boiling in sodium citrate (pH 6.0) then blocked with 10% normal goat serum. Sections were then incubated overnight at 4°C with anti-PSAT1 antibody (1:200; Novus Biologicals) antibody. Sections were washed, blocked, incubated with biotinylated anti-rabbit secondary antibody (Vector Laboratories, Inc.) and then incubated with avidin–biotin complex reagent (Vector Laboratories, Inc.) for 30 minutes at room temperature, followed by signal detection with 3,30-diaminobenzidine solution (Vector Laboratories). Tissues were counterstained with hematoxylin. The study was approved by the WCM Institutional Review Board.

Survival analysis

To determine whether there is an association between serine synthesis gene expression and patient survival in the TCGA dataset, joint measures of *PHGDH*, *PSAT1* and *PSPH* expression were used to group patients into high or low gene expression. Since these genes are not in perfect correlation with each other, a probabilistically-motivated method for assignment to “high” or “low” groups was devised. First, the expression values of the three genes were averaged. This value was then split into a “high” or “low” group based on an

adaptive threshold value. The threshold value was picked such that there was maximum concordance between the final assigned groups and the original average gene expression values using a Somer's D-based calculation. This was achieved by pooling all individual group comparisons into a single D calculation. The value was then normalized as D/sqrt(var(D)), where var(D) was computed using an infinitesimal jackknife estimator as described in (30). The threshold for grouping the averaged gene expression values was then picked at the value that maximizes this normalized D measure, thus resulting in an optimized separation of patients into high or low groups (Supplementary Fig. S1A&B). A log-rank test was used to determine if these gene expression groups correlated with survival.

Statistical analysis

For gene expression data of the three genes of interest extracted from GSE8671 or generated in mouse experiments, differences in gene expression between polyp and adjacent normal tissue was compared using Wilcoxon signed-rank test. For relative cell number measured as fold change from day 0, linear regression was used to model the relative cell number (square root transformed) as a function of treatment group, time and their interactions. Simultaneous testing of general linear hypotheses was used to compare the relative cell number growth rates between pairs of experimental conditions. P-values were adjusted for multiple comparisons using the Bonferroni-Holm method. Linear mixed-effects model with experimental group, time and group by time interaction as fixed effects and mouse specific random intercept was used to fit the longitudinal tumor volume (log transformed) data. Differences in tumor growth rates were examined using simultaneous tests for general linear hypotheses of contrasts of interest. For tumor volume (log transformed) measured at the end of experiment, differences across experimental groups was examined using ANOVA followed by simultaneous tests for general linear hypotheses of contrasts of interest. P-values were adjusted for multiple comparisons using the Bonferroni-Holm method. Differences in the proportion of mice with a decrease in tumor volume following 11 days of 5 FU treatment was examined using Fisher's exact test. Welch's t-test was used to examine the difference in percent of 53BP1 foci positive cells (log transformed) between the two experimental groups. ANOVA was used to examine the difference in cell viability percent across experimental groups. Differences for contrasts of interest were evaluated using simultaneous tests for general linear hypotheses. P-values were adjusted for multiple comparisons by using Tukey's method for pairwise comparisons or Bonferroni-Holm approach for other contrasts. For data analyzed using parametric approaches, data transformation as noted for each endpoint was used to ensure the underlying model assumptions were satisfied.

Results

High serine synthesis gene expression correlates with poor survival in colon cancer patients

The established growth-promoting role of serine in cancer cells, previous evidence that serine levels are increased in colon cancer and the finding that increased expression of genes controlling serine synthesis enhances xenograft growth, suggest that this pathway plays a role in the progression of colon cancer (1–3,8,10,22,23). To begin to examine this concept,

we mined data from TCGA to evaluate whether there was a correlation between expression of genes controlling serine synthesis and survival of colon cancer patients. Based on an analysis of 265 tumors, high *vs.* low expression of genes responsible for serine synthesis was associated with reduced overall survival (Hazard ratio = 1.71 (95% CI) [2.89, 1.01]; P=0.042) (Supplementary Figs. S1A&B & S2A; Supplementary Table S4). We further interrogated these data to evaluate whether *KRAS* mutational status impacts this association. Interestingly, when *KRAS* WT vs. mutant tumors were examined separately, reduced survival associated with high serine synthesis gene expression occurred exclusively in patients with *KRAS* mutant tumors (Hazard ratio = 2.56 (95% CI) [5.51, 1.19]; P=0.013 for patients with *KRAS* mutant tumors) (Supplementary Fig. S2B&C).

APC status controls the expression of serine synthesis genes in murine intestinal polyps

We next investigated potential pathways controlling serine synthesis in CRC using murine models. Previous work has shown that activated Wnt signaling can induce the expression of serine synthesis genes in several neoplastic cell types (18–20,31). This effect appears to stem from increased binding of Myc to E-box sequences in the promoters of these genes (20,31). Given these observations and the fact that *APC* mutations are common in intestinal neoplasia, resulting in activation of Wnt signaling (21), we reasoned that *APC* status would impact the expression of genes controlling serine synthesis in intestinal neoplasms. To test this possibility, we first examined intestinal polyps arising in $Apc^{Min/+}$ mice, in which tumors develop as a result of loss of *Apc* (32). Here, we found marked increases in *Phgdh* and *Psat1* expression compared to normal intestinal mucosa from WT mice (Fig. 1A). Second, we utilized a mouse model carrying an inducible shRNA targeting *Apc*, which upon activation, reduces *Apc* expression in the colon (33). This model demonstrated that the expression of genes encoding enzymes from the serine synthesis pathway increased upon *Apc* suppression, an effect that was reversed upon re-expression of *Apc* (Fig. 1B). Given prior evidence that *Kras* mutations can augment the expression of genes involved in serine synthesis resulting from loss of APC (12), we next determined the effect of the addition of *Kras* mutations in the *shApc* mouse ($shApc/Kras^{G12D}$). As shown in Figure 1C, the magnitude of increase of serine synthesis gene expression was nearly identical in $shApc/Kras^{G12D}$ and *shApc* mice, relative to normal mucosa from control *shRen* mice. Consistent with these murine findings, examination of TCGA data showed no impact of *KRAS* mutation status on the expression of serine synthesis genes in human colon tumors (Supplementary Fig. S3). These findings suggest that *APC* status may impact serine synthesis in intestinal neoplasia, an effect that is not enhanced by *KRAS* mutations.

Increased PSAT1 expression in benign and malignant human colon tumors.

Given the findings shown above which support the potential importance of the serine synthesis pathway in both premalignant adenomas and adenocarcinomas of the colon, further studies were carried out to better understand the role of this pathway in CRC pathogenesis. First, gene expression was interrogated in colon adenomas using publicly available data in 32 paired samples of polyps and normal mucosa (34). Significant increases in *PHGDH* and *PSAT1* were found in adenomatous polyps compared to normal tissue (Fig. 2A). Further analysis in these samples showed that *PSAT1* was the most strongly (P<0.001) and consistently increased gene as compared to *PHGDH* and *PSPH* (Fig. 2B). To confirm

these findings at the protein level, we utilized immunohistochemistry (IHC) which revealed that PSAT1 is strongly increased in the cytoplasm of the epithelial cells in adenomas compared to normal adjacent tissues (Fig. 2C). To evaluate whether PSAT1 was also increased in adenocarcinomas, western blotting was performed. As shown in Figure 2D, PSAT1 protein levels were increased in tumors compared to normal adjacent mucosa in 10 paired samples. Immunohistochemistry confirmed that levels of PSAT1 are elevated in the cytoplasm of cancer cells compared to normal adjacent tissues (Fig. 2E). Taken together, these findings strongly suggest a role for increased serine biosynthesis in CRC pathogenesis, and the potential relevance for PSAT1 as a mediator in these processes.

Reducing availability of both endogenous and exogenous serine maximally suppresses colon cancer cell proliferation

Given the potential importance of PSAT1 in colonic neoplasia (Fig. 2), we deleted *PSAT1* in human HCT116 and DLD1 colon cancer cell lines to evaluate the biological effects associated with its loss. To accomplish this, we utilized a CRISPR-based gene editing approach. Successful gene editing of PSAT1 was confirmed by T7 surveyor assay using three different guide RNAs (Supplementary Fig. S4). Western blot analysis confirmed the loss of PSAT1 protein expression in these cell lines compared to cells expressing an empty vector (EV) (Fig. 3A). Using these cells, we first evaluated the effects of *PSAT1* deletion alone, exogenous serine removal alone or their combination on cell proliferation by flow cytometry-based cell counting. As shown in Fig. 3B, over a 4 day period, deletion of *PSAT1* alone (PSAT1KO Comp) had no effect on cell proliferation in HCT116 cells and only a modest inhibitory effect in DLD1 cells, compared to EV cells grown in complete medium (EV Comp). As expected, removing serine from the medium of EV cells (EV Ser Def) strongly suppressed cell proliferation in both cell lines (Fig. 3B). Notably, combining serine removal from the medium and *PSAT1* deletion (PSAT1KO Ser Def) maximally suppressed cell growth (Fig. 3B). Taken together, these findings suggest that although CRC cells in culture largely rely on exogenous serine to support their proliferation, they depend on serine synthesis when exogenous serine is removed.

PSAT1 deletion enhances metabolic defects in serine-deprived HCT116 and DLD1 cells

We next sought to determine how limiting different sources of serine impacted cellular metabolism which might contribute, in turn, to the proliferative defect we observed (Fig. 3B). Therefore, we carried out metabolite profiling in the EV Comp, PSAT1KO Comp, EV Ser Def and PSAT1KO Ser Def groups following 12 hr of culture. Principal component analysis revealed that EV Ser Def cells clustered strongly away from EV Comp cells along the PC1 while PSAT1KO Ser Def cells also shifted away from the EV Comp group with an additional shift along the PC2 (Fig. 3C). PSAT1KO Comp cells clustered relatively close to the EV Comp group (Fig. 3C). Analysis of metabolite changes comparing EV Comp to the other 3 groups revealed that the relative abundance of 71 metabolites was significantly altered in the EV Ser Def group while 111 were significantly changed in PSAT1KO Ser Def cells (Fig. 3D; Supplementary Table S5). Of those metabolites that significantly changed in both EV Ser Def and PSAT1KO Ser Def groups, 25 had a greater magnitude of change in the PSAT1KO Ser Def cells compared to EV Ser Def (Fig. 3D; Supplementary Table S5). The only significantly changed metabolite in PSAT1KO Comp cells was phosphoserine, the

immediate product of PSAT1 activity, which showed a decrease (P<0.001). Of note, intracellular serine levels were significantly reduced in EV Ser Def cells (P<0.01), with a trend for a more robust decrease in PSAT1KO Ser Def cells (P=0.08) (Supplementary Fig. S5).

Aggregation-based analysis of the metabolite profile to inform on pathway changes revealed a marked decrease in nucleotide-related molecules in both EV and PSAT1KO cells grown in serine deficient medium (Fig. 3E). Hence, we next looked in greater depth at the abundance of specific metabolites relevant for this pathway in each of the four conditions. We found that 5-Aminoimidazole-4-carboxamide riboside (AICAR), a precursor for *de novo* purine synthesis, was dramatically increased in the EV Ser Def and PSAT1KO Ser Def groups indicating impaired nucleotide synthesis (Fig. 3F). In association with this change, Inosine monophosphate (IMP), Adenosine monophosphate (AMP) and 2'-deoxyguanosine 5'-monophosphate (dGMP) abundance were altered (Fig. 3F). Thymidine monophosphate (TMP) and Thymidine 5-triphosphate (TTP), two important mediators of cancer cell proliferation, were decreased in EV Ser Def cells, an effect that was enhanced in the PSAT1KO Ser Def group (P=0.051 and 0.1 for TMP and TTP, respectively *vs.* EV Ser Def) (Fig. 3F). Despite such a defect in nucleotide production, cells did not switch to nucleotide salvage as an adaptive response, as determined by lack of incorporation of labeled hypoxanthine into nucleotides (Supplementary Fig. S6). Interestingly, PSAT1 deletion alone did not alter the incorporation of exogenous serine into nucleotides, based on evaluating incorporation of labeled serine (Supplementary Fig. S7). Of note, a very similar pattern of metabolite changes occurred in the DLD1 cell line, although these were not as pronounced as what was observed in HCT116 cells (Supplementary Fig. S8A & Supplementary Table S6). These included 45 metabolites significantly altered in PSAT1KO Ser Def cells and 8 significant changes in EV Ser Def conditions, 7 of which overlap with the PSAT1KO Ser Def group (Supplementary Fig. S8B & Supplementary Table S6). No significant changes were observed in PSAT1KO Comp cells. Aggregation analysis suggested nucleotide-related molecules were selectively changed in PSAT1KO Ser Def cells (P=0.096), with associated alterations in key metabolites in this pathway (Supplementary Fig. S8C & D). Altogether these findings indicate that limiting both sources of serine maximally perturbs cancer cell metabolism with profound effects on nucleotides.

Distinct gene expression changes occur when both sources of serine are eliminated

Thus far, we demonstrated that restricting endogenous and exogenous sources of serine more profoundly suppresses tumor cell proliferation and induces metabolic defects compared to removing exogenous serine alone. Next, we investigated whether loss of both sources of serine resulted in a unique gene expression pattern compared to only removing serine in the medium. To evaluate this, we carried out RNA-seq on EV Comp, EV Ser Def and PSAT1KO Ser Def HCT116 cells after 24 hr of culture. Clustering analysis of gene expression differences showed clear separation across the groups (Fig. 4A). These differences included nearly 3,000 gene expression changes in the EV Ser Def group with an additional ~800 changes occurring in the PSAT1KO Ser Def group, when comparing either group to EV Comp cells (Fig. 4A). The majority of genes decreased in expression in both groups with more than 1,000 distinct genes following this pattern in PSAT1KO Ser Def cells (Fig. 4B).

Among upregulated genes, approximately 250 were selectively changed in the PSAT1KO Ser Def group (Fig. 4B). In order to elucidate pathways associated with gene expression changes under serine-deprived conditions, we carried out gene set enrichment analysis using KEGG pathways. A comparison of the gene expression changes that occurred in the EV Ser Def and PSAT1KO Ser Def groups compared to EV Comp cells revealed upregulated pathways associated with DNA replication and repair and downregulated pathways associated with cancer (Fig. 4C).

Serine restriction induces a DNA damage response that can be inhibited with formate

The metabolic defects (nucleotide imbalance) and gene expression patterns (increased nucleotide excision repair, base excision repair, etc.) observed upon serine restriction suggest a correlation between reduced nucleotide production and a DNA damage response. In fact, previous work has shown that a reduced nucleotide pool and nucleotide imbalances favor DNA damage (35). To determine whether a DNA damage response occurred under serine-deprived conditions, we first tested for the presence of phosphorylated histone 2AX (γH2AX), a marker of double stranded DNA breaks, in HCT116 cells. As shown in Figure 4D (top), there was a minimal accumulation of γH2AX when only exogenous serine was removed, however, a robust increase was observed when both sources of serine were targeted. To confirm the occurrence of DNA damage under this condition, immunofluorescence staining for tumor suppressor p53 binding protein 1 (53BP1) was carried out. As shown in Figure 4D (middle & bottom), removal of both sources of serine resulted in a marked increase in 53BP1 positive foci. A similar increase in 53BP1 staining was observed in DLD1 cells (Supplementary Fig. S9). Because serine utilization leads to formate production by mitochondria to support nucleotide synthesis and cell proliferation, we reasoned that adding back exogenous formate would protect against this DNA damage and impaired proliferation (1–3,10). As shown in Fig. 4E & F, addition of 1mM formate strongly attenuated the increase in the DNA damage response and completely rescued the cell proliferation defect in PSAT1KO Ser Def cells. Formate supplementation afforded similar protective effects from DNA damage and impaired proliferation in DLD1 cells (Supplementary Fig. S10A&B).

Combining dietary serine removal and PSAT1 deletion is necessary to suppress tumor growth

Thus far our work has demonstrated a role for exogenous and endogenous sources of serine in supporting CRC cell proliferation and metabolism *in vitro*. To determine whether reducing either or both sources of serine impacts tumor growth, we injected HCT116 EV, HCT116 PSAT1 KO, DLD1 EV and DLD1 PSAT1KO cells into the flanks of athymic, immunodeficient mice and fed them either complete amino acid-based diet or a serine-deficient diet. Measurements of tumor volume over a period of 4–6 weeks following injection revealed that neither *PSAT1* deletion nor feeding a serine deficient diet alone significantly impacted tumor growth (Fig. 5A and B). However, removing serine from the diet led to a significant suppression of growth of both HCT116 and DLD1 xenografts when *PSAT1* was deleted (Fig. 5A and B). Consistent with these findings, the size of tumors derived from PSAT1KO cells from mice fed serine deficient diet were also markedly smaller

at the final time point (Fig. 5C and D). Taken together, these data suggest that it is necessary to restrict both sources of serine to optimally suppress the growth of CRC *in vivo*.

5-FU reduces tumor size under serine-deprived conditions

Given the impaired nucleotide production and increase in DNA damage occurring in PSAT1KO Ser Def cells (Figs. 3 & 4), we reasoned that such a stressed state may render cells more susceptible to chemotherapy. 5-FU is a chemotherapeutic agent used as part of frontline therapy for most CRC patients, with a major mechanism of action being induction of nucleotide imbalances and DNA damage, leading to cell death (36). To test the effects of 5-FU under serine-deprived conditions, nude mice were injected with EV or PSAT1KO HCT116 cells into their flanks and given complete diet while tumors were allowed to grow to a palpable size. Mice bearing tumors were then divided into 4 groups: 1) EV tumors given Comp diet and vehicle, 2) EV tumors given Comp diet and 75mg/kg 5-FU, 3) PSAT1KO tumors given Ser Def diet and vehicle, 4) PSAT1KO tumors given Ser Def diet and 75mg/kg 5-FU. Injections of vehicle or 5-FU were given intraperitoneally every 3–4 days over an 11 day period. In the presence of a complete diet, 5-FU suppressed the growth of HCT116 EV xenografts ($P<0.001$) (Fig. 6A). In contrast, treatment with 5-FU led to a reduction in size of HCT116 PSAT1KO xenografts when mice were given a serine deficient diet (Fig. 6A). A significantly larger percent of HCT116 tumors were reduced in size in response to 5-FU in the PSAT1KO Ser Def group (100%) compared to the EV Comp group (38%) ($P<0.001$) (Fig. 6B).

To examine the potential mechanism underlying the anti-tumor effect of 5-FU in these conditions, EV and PSAT1KO cells were grown *in vitro* in the presence or absence of serine, respectively, and treated with multiple concentrations of 5-FU or vehicle. Significantly greater cell death was observed in the PSAT1KO Ser Def group treated with 5-FU after 4 days compared to the EV Comp group (Fig. 6C). We next carried out metabolite profiling in cells treated with 1.5μM 5-FU or vehicle after 1 day of treatment to gain insight into what metabolic changes might account for the observed increase in cell death. Nine metabolites were identified when determining which mediators were significantly altered in abundance comparing PSAT1KO Ser Def cells treated with 5-FU to each of the other 3 groups and of the highest or lowest abundance compared to each of the other 3 groups (Fig. 6D; Supplementary Table S7). Among them, the key nucleotides TMP and TTP were markedly reduced (Fig. 6D). Interestingly, these metabolic changes were associated with a markedly enhanced DNA damage response following 5-FU treatment in the PSAT1KO Ser Def group (Fig. 6E). Finally, we demonstrated that formate supplementation protected against cell death following 5-FU treatment of PSAT1KO Ser Def cells, indicating that the enhanced susceptibility to this drug was due to formate depletion (Fig. 6F).

Discussion

Serine utilization by cancer cells is believed to contribute to cell proliferation and tumor growth. However, the importance of exogenous *vs.* endogenous sources of serine as determinants of colorectal cancer biology is not well understood. This study demonstrated that levels of PSAT1, a key enzyme in serine biosynthesis, are elevated in colorectal

adenomas and adenocarcinomas. In cultured colon cancer cells, *PSAT1* deletion enhanced the growth-suppressive effects of removing serine from the medium. These effects were accompanied by reduced nucleotide production and increased DNA damage. *In vivo*, restricting both endogenous serine biosynthesis (PSAT1 KO) and dietary serine was required to significantly suppress tumor growth. Moreover, the anti-tumor activity of 5-FU was enhanced when both serine and dietary sources of serine were removed. These findings support the possibility that restricting both sources of serine could be beneficial for limiting colon tumor growth and augmenting the efficacy of 5-FU for the treatment of CRC patients.

Pioneering work from Vousden and Maddocks established that CRC cells prefer to utilize serine instead of glycine and demonstrated the reliance of these cells on exogenous serine uptake to fuel tumor cell proliferation and several aspects of cellular metabolism (11,37,38). Moreover, this work demonstrated that cells upregulate the expression of serine synthesis enzymes upon exogenous serine removal, suggesting that they switch to synthesis under serine deplete conditions (11). Our *in vitro* findings further support the importance of exogenous serine for colon cancer cell proliferation, but the fact that *PSAT1* deletion enhanced the anti-proliferative and metabolic effects of removing exogenous serine suggests that tumor cells rely on serine synthesis when exogenous serine is not available. However, given the fact that cells restricted of both sources of serine still proliferated, albeit slowly, suggests that redundant aminotransferases may partially fulfill the role of PSAT1 under these conditions. Regardless, the observation that deleting *PSAT1* alone had a minimal effect on cell proliferation demonstrates that cells in culture rely heavily on exogenous serine. Both of these findings are supported by recent work showing that reduced PHGDH expression is only effective at slowing cancer cell proliferation under low serine conditions (17).

Although an *in vitro* system is useful for determining the potential importance of endogenous and exogenous sources of serine for regulating tumor cell proliferation, the concentration of amino acids in culture media far exceeds physiologic levels (39). Therefore, *in vivo* experiments are necessary to more accurately evaluate the contributions of exogenous and endogenous serine to cancer cell growth. To this end, we found essentially no effect on tumor growth after either *PSAT1* deletion in tumor cells or eliminating serine from the diet. However, the combination of deleting *PSAT1* and feeding a serine-free diet clearly inhibited tumor growth. Previous *in vivo* work demonstrated that removal of both serine and glycine from the diet suppressed xenograft growth and increased survival in mice bearing intestinal polyps (11,12). However, five additional amino acids were excluded from the diet in these studies (11,12). In our study, we elected to remove only serine from diet in order to solely examine its contribution. Certainly, including all other amino acids besides serine in the serine deficient diet used in our work could account for the difference in effect on tumor growth between the studies in a PSAT1 sufficient state. In fact, recent studies using a serine and glycine deficient diet that included all other amino acids, showed no effect on tumor growth in mice when cells were serine synthesis competent (15,17). Interestingly, one of these studies showed that combining *Psat1* deletion with a serine/glycine deficient diet was necessary to slow murine liver tumor growth (15). Examining whether loss of both serine sources at early stages in a murine colon cancer model slows or prevents tumor growth warrants investigation in future studies.

Serine is an important contributor to one-carbon metabolism, a complex pathway that impacts several aspects of cellular physiology and supports oncogenesis (1–3,10). The one-carbon unit generated by serine metabolism is utilized in the mitochondria through a series of reactions resulting in the release of formate into the cytosol (1–3,10). Metabolism of cytosolic formate is critical for the production of nucleotides to support cell proliferation (1–3,10). Metabolite profiling of EV and PSAT1KO cells under serine-restricted conditions showed a marked depletion in nucleotides, an effect that was associated with a DNA damage response as indicated by gene expression changes and increased H2AX phosphorylation and 53BP1foci formation. In fact, it is known that nucleotide imbalances can promote the DNA damage response (35). Our data further demonstrate that it is the generation of formate that is a key mechanism by which serine prevents this DNA damage response and concomitantly supports cell proliferation (Fig. 4E & F; Supplementary Fig. S10). These findings are supported by previous evidence that exogenous restriction of either both serine and glycine or only serine reduced intracellular nucleotide levels, an effect that was associated with suppressed proliferation (11,37). Moreover, exogenous formate rescued the defect in proliferation following serine removal which correlated with enhanced nucleotide production (37). That said, it should be noted that addition of formate could also restore serine levels, which might account for its protective effects (40). Restriction of exogenous and endogenous serine sources in the current work led to greater suppression of cell proliferation and enhanced nucleotide alterations compared with exogenous serine removal alone, effects associated with an augmented DNA damage response. Therefore, the ability of cancer cells to adapt to a low serine environment by switching to synthesis is critical to maintain proper cell function. Interestingly, gene expression analysis under the same conditions suggest that reduced nucleotide pools results in an apparent compensatory increase in expression of genes involved in DNA replication and purine metabolism (Fig. 4C). It is also logical to predict that changes in other classes of molecules such as lipids may likewise be enhanced under these conditions (13).

Our findings led to the hypothesis that the metabolic changes (e.g., reduced nucleotide levels) and increased DNA damage resulting from serine deficiency, might sensitize cells to chemotherapy. To this end, we demonstrated that 5-FU, a commonly used chemotherapeutic drug in CRC patients, caused a reduction in 100% of xenografts derived from PSAT1KO cells in mice fed a serine deficient diet, whereas the same treatment caused only modest reduction in a minority of EV cell-derived xenografts in mice fed a serine replete diet. Along these lines, the effect of a serine- and glycine-deficient diet on the anti-tumor response of phenformin and metformin was tested in lymphoma and intestinal tumor models, respectively (12). These drugs enhanced survival when used in combination with a serine and glycine deficient diet in both models and reduced tumor number in $Apc^{Min/+}$ mice (12). We elected to test 5-FU given its common use as part of frontline treatment for CRC patients. 5-FU, an analogue of uracil, functions by both incorporating into RNA and inhibiting thymidylate synthetase (the key enzyme to produce TMP) (36). The latter mechanism results in profound nucleotide imbalances and DNA damage, which can lead to cell death (36). Our mechanistic studies demonstrated that low dose 5-FU induced a much more dramatic increase in DNA damage in PSAT1KO Ser Def cells compared to the EV Comp group, suggesting more severe DNA damage in the context of serine deficiency.

Metabolite profiling identified nine metabolites that were selectively altered in abundance following 5-FU treatment in PSAT1KO cells grown in serine deficient, including reduced levels of the key nucleotides TMP and TTP. Interestingly, the addition of formate protected PSAT1KO Ser Def cells from 5-FU induced death, suggesting a key role for serine-derived formate for protecting against 5-FU induced cytotoxicity. These data support the concept that combining restriction of both sources of serine and exposure to 5-FU severely impairs DNA replication and repair and maximally induces DNA damage, resulting in intracellular catastrophic events leading to death.

Supplementary Material

Refer to Web version on PubMed Central for supplementary material.

Acknowledgments:

D.C.M. is supported by NIH/NCI K22CA226033, Prevent Cancer Foundation grant, Weill Department of Medicine Seed Grant for Innovative Research, and startup funds from the Stony Brook Cancer Center and Bahl Center for Metabolomics and Imaging. L.G. is supported by a Breakthrough Level 2 grant from the US Department of Defense (DoD), Breast Cancer Research Program (BRCP) (#BC180476P1), the 2019 Laura Ziskin Prize in Translational Research (#ZP-6177, PI: Formenti) from the Stand Up to Cancer (SU2C), a Mantle Cell Lymphoma Research Initiative (MCL-RI, PI: Chen-Kiang) grant from the Leukemia and Lymphoma Society (LLS), a startup grant from the Dept. of Radiation Oncology at Weill Cornell Medicine (New York, US), a Rapid Response Grant from the Functional Genomics Initiative (New York, US), by industrial collaborations with Lytix (Oslo, Norway) and Phosplatin (New York, US), and by donations from Phosplatin (New York, US), the Luke Heller TECPR2 Foundation (Boston, US) and Sotio a.s. (Prague, Czech Republic).

References

1. Locasale JW. Serine, glycine and one-carbon units: cancer metabolism in full circle. Nat Rev Cancer 2013;13:572–83 [PubMed: 23822983]
2. Mattaini KR, Sullivan MR, Vander Heiden MG. The importance of serine metabolism in cancer. J Cell Biol 2016;214:249–57 [PubMed: 27458133]
3. Yang M, Vousden KH. Serine and one-carbon metabolism in cancer. Nat Rev Cancer 2016;16:650–62 [PubMed: 27634448]
4. DeNicola GM, Chen PH, Mullarky E, Sudderth JA, Hu Z, Wu D, et al. NRF2 regulates serine biosynthesis in non-small cell lung cancer. Nat Genet 2015;47:1475–81 [PubMed: 26482881]
5. Locasale JW, Grassian AR, Melman T, Lyssiotis CA, Mattaini KR, Bass AJ, et al. Phosphoglycerate dehydrogenase diverts glycolytic flux and contributes to oncogenesis. Nat Genet 2011;43:869–74 [PubMed: 21804546]
6. Possemato R, Marks KM, Shaul YD, Pacold ME, Kim D, Birsoy K, et al. Functional genomics reveal that the serine synthesis pathway is essential in breast cancer. Nature 2011;476:346–50 [PubMed: 21760589]
7. Reid MA, Allen AE, Liu S, Liberti MV, Liu P, Liu X, et al. Serine synthesis through PHGDH coordinates nucleotide levels by maintaining central carbon metabolism. Nat Commun 2018;9:5442 [PubMed: 30575741]
8. Vie N, Copois V, Bascoul-Mollevi C, Denis V, Bec N, Robert B, et al. Overexpression of phosphoserine aminotransferase PSAT1 stimulates cell growth and increases chemoresistance of colon cancer cells. Mol Cancer 2008;7:14 [PubMed: 18221502]
9. Yang Y, Wu J, Cai J, He Z, Yuan J, Zhu X, et al. PSAT1 regulates cyclin D1 degradation and sustains proliferation of non-small cell lung cancer cells. Int J Cancer 2015;136:E39–50 [PubMed: 25142862]
10. Ducker GS, Rabinowitz JD. One-Carbon Metabolism in Health and Disease. Cell Metab 2017;25:27–42 [PubMed: 27641100]

11. Maddocks OD, Berkers CR, Mason SM, Zheng L, Blyth K, Gottlieb E, et al. Serine starvation induces stress and p53-dependent metabolic remodelling in cancer cells. Nature 2013;493:542–6 [PubMed: 23242140]
12. Maddocks ODK, Athineos D, Cheung EC, Lee P, Zhang T, van den Broek NJF, et al. Modulating the therapeutic response of tumours to dietary serine and glycine starvation. Nature 2017;544:372–6 [PubMed: 28425994]
13. Gao X, Lee K, Reid MA, Sanderson SM, Qiu C, Li S, et al. Serine Availability Influences Mitochondrial Dynamics and Function through Lipid Metabolism. Cell Rep 2018;22:3507–20 [PubMed: 29590619]
14. Ye J, Mancuso A, Tong X, Ward PS, Fan J, Rabinowitz JD, et al. Pyruvate kinase M2 promotes de novo serine synthesis to sustain mTORC1 activity and cell proliferation. Proc Natl Acad Sci U S A 2012;109:6904–9 [PubMed: 22509023]
15. Mendez-Lucas A, Lin W, Driscoll PC, Legrave N, Novellasdemunt L, Xie C, et al. Identifying strategies to target the metabolic flexibility of tumours. Nat Metab 2020;2:335–50 [PubMed: 32694609]
16. Mullarky E, Lucki NC, Beheshti Zavareh R, Anglin JL, Gomes AP, Nicolay BN, et al. Identification of a small molecule inhibitor of 3-phosphoglycerate dehydrogenase to target serine biosynthesis in cancers. Proc Natl Acad Sci U S A 2016;113:1778–83 [PubMed: 26831078]
17. Sullivan MR, Mattaini KR, Dennstedt EA, Nguyen AA, Sivanand S, Reilly MF, et al. Increased Serine Synthesis Provides an Advantage for Tumors Arising in Tissues Where Serine Levels Are Limiting. Cell Metab 2019;29:1410–21 e4 [PubMed: 30905671]
18. Sun L, Song L, Wan Q, Wu G, Li X, Wang Y, et al. cMyc-mediated activation of serine biosynthesis pathway is critical for cancer progression under nutrient deprivation conditions. Cell Res 2015;25:429–44 [PubMed: 25793315]
19. Walther N, Ulrich A, Vockerodt M, von Bonin F, Klapper W, Meyer K, et al. Aberrant lymphocyte enhancer-binding factor 1 expression is characteristic for sporadic Burkitt's lymphoma. Am J Pathol 2013;182:1092–8 [PubMed: 23375451]
20. Marinkovic D, Marinkovic T, Kokai E, Barth T, Moller P, Wirth T. Identification of novel Myc target genes with a potential role in lymphomagenesis. Nucleic Acids Res 2004;32:5368–78 [PubMed: 15477387]
21. Kwong LN, Dove WF. APC and its modifiers in colon cancer. Adv Exp Med Biol 2009;656:85–106 [PubMed: 19928355]
22. Hirayama A, Kami K, Sugimoto M, Sugawara M, Toki N, Onozuka H, et al. Quantitative metabolome profiling of colon and stomach cancer microenvironment by capillary electrophoresis time-of-flight mass spectrometry. Cancer Res 2009;69:4918–25 [PubMed: 19458066]
23. Montrose DC, Zhou XK, Kopelovich L, Yantiss RK, Karoly ED, Subbaramaiah K, et al. Metabolic profiling, a noninvasive approach for the detection of experimental colorectal neoplasia. Cancer Prev Res (Phila) 2012;5:1358–67 [PubMed: 22961778]
24. Zafra MP, Schatoff EM, Katti A, Foronda M, Breinig M, Schweitzer AY, et al. Optimized base editors enable efficient editing in cells, organoids and mice. Nat Biotechnol 2018;36:888–93 [PubMed: 29969439]
25. Dow LE, Fisher J, O'Rourke KP, Muley A, Kastenhuber ER, Livshits G, et al. Inducible in vivo genome editing with CRISPR-Cas9. Nat Biotechnol 2015;33:390–4 [PubMed: 25690852]
26. Dieterle F, Ross A, Schlotterbeck G, Senn H. Probabilistic quotient normalization as robust method to account for dilution of complex biological mixtures. Application in 1H NMR metabonomics. Anal Chem 2006;78:4281–90 [PubMed: 16808434]
27. Benjamini Y, Hochberg Y. Controlling the False Discovery Rate: a Practical and Powerful Approach to Multiple Testing. J R Statist Soc B 1995;57:289–300
28. Krumsiek J, Mittelstrass K, Do KT, Stuckler F, Ried J, Adamski J, et al. Gender-specific pathway differences in the human serum metabolome. Metabolomics 2015;11:1815–33 [PubMed: 26491425]
29. Chen Q, Kirk K, Shurubor YI, Zhao D, Arreguin AJ, Shahi I, et al. Rewiring of Glutamine Metabolism Is a Bioenergetic Adaptation of Human Cells with Mitochondrial DNA Mutations. Cell Metab 2018;27:1007–25 e5 [PubMed: 29657030]

30. Therneau TMW DA The concordance statistic and the Cox model. Department of Health Science Research Mayo Clinic Technical Report 2017;85:1–18

31. Xia Y, Ye B, Ding J, Yu Y, Alptekin A, Thangaraju M, et al. Metabolic Reprogramming by MYCN Confers Dependence on the Serine-Glycine-One-Carbon Biosynthetic Pathway. Cancer Res 2019;79:3837–50 [PubMed: 31088832]

32. Su LK, Kinzler KW, Vogelstein B, Preisinger AC, Moser AR, Luongo C, et al. Multiple intestinal neoplasia caused by a mutation in the murine homolog of the APC gene. Science 1992;256:668–70 [PubMed: 1350108]

33. Dow LE, O'Rourke KP, Simon J, Tschaharganeh DF, van Es JH, Clevers H, et al. Apc Restoration Promotes Cellular Differentiation and Reestablishes Crypt Homeostasis in Colorectal Cancer. Cell 2015;161:1539–52 [PubMed: 26091037]

34. Sabates-Bellver J, Van der Flier LG, de Palo M, Cattaneo E, Maake C, Rehrauer H, et al. Transcriptome profile of human colorectal adenomas. Mol Cancer Res 2007;5:1263–75 [PubMed: 18171984]

35. Turgeon MO, Perry NJS, Poulogiannis G. DNA Damage, Repair, and Cancer Metabolism. Front Oncol 2018;8:15 [PubMed: 29459886]

36. Longley DB, Harkin DP, Johnston PG. 5-fluorouracil: mechanisms of action and clinical strategies. Nat Rev Cancer 2003;3:330–8 [PubMed: 12724731]

37. Labuschagne CF, van den Broek NJ, Mackay GM, Vousden KH, Maddocks OD. Serine, but not glycine, supports one-carbon metabolism and proliferation of cancer cells. Cell Rep 2014;7:1248–58 [PubMed: 24813884]

38. Maddocks OD, Labuschagne CF, Adams PD, Vousden KH. Serine Metabolism Supports the Methionine Cycle and DNA/RNA Methylation through De Novo ATP Synthesis in Cancer Cells. Mol Cell 2016;61:210–21 [PubMed: 26774282]

39. Cantor JR, Abu-Remaileh M, Kanarek N, Freinkman E, Gao X, Louissaint A Jr., et al. Physiologic Medium Rewires Cellular Metabolism and Reveals Uric Acid as an Endogenous Inhibitor of UMP Synthase. Cell 2017;169:258–72 e17 [PubMed: 28388410]

40. Tan YL, Sou NL, Tang FY, Ko HA, Yeh WT, Peng JH, et al. Tracing Metabolic Fate of Mitochondrial Glycine Cleavage System Derived Formate In Vitro and In Vivo. Int J Mol Sci 2020;21

Statement of Significance

These findings provide insights into the metabolic requirements of colorectal cancer and reveal a novel approach for its treatment.

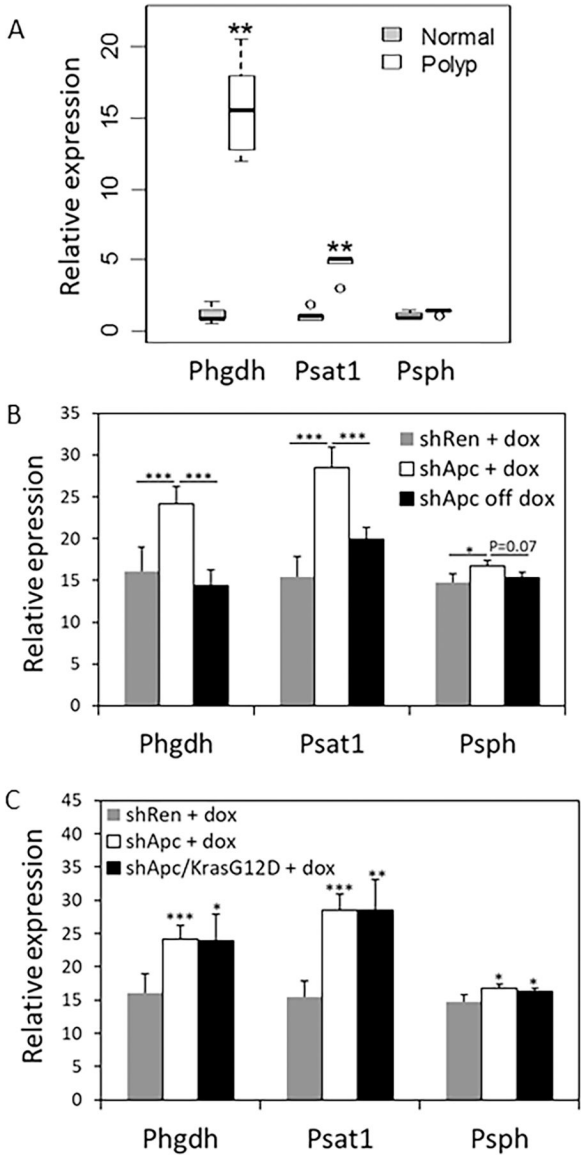

Figure 1.

APC status impacts serine synthesis gene expression in murine intestinal tumors. (A) The expression of *Phgdh*, *Psat1* and *Psph* was compared in ileal polyps from $Apc^{Min/+}$ mice *vs.* normal ileal mucosa from WT mice by qRT-PCR. Gene expression in polyps was calculated relative to normal mucosa (n=5 per group). **P<0.01 compared to normal tissue for each gene. (B) Expression levels of *Phgdh*, *Psat1* and *Psph* were determined by RNA seq in colonic tissue from *shRen* mice given doxycycline for 15 weeks (*shRen* + dox), *shApc* mice given doxycycline for 15 weeks (*shApc* + dox) and *shApc* mice 4 days following doxycycline removal (*shApc* off dox) (n=4 per group). *P<0.05; ***P<0.001 as indicated. (C) Expression levels of *Phgdh*, *Psat1* and *Psph* were determined by RNA seq in colonic tissue from *shApc/KrasG12D* mice given doxycycline for 15 weeks and shown along with data found in panel B from the *shRen* + dox and *shApc* + dox groups (n=4 per group). *P<0.05; **P<0.01; ***P<0.001 compared to the *shRen* group for each gene as indicated.

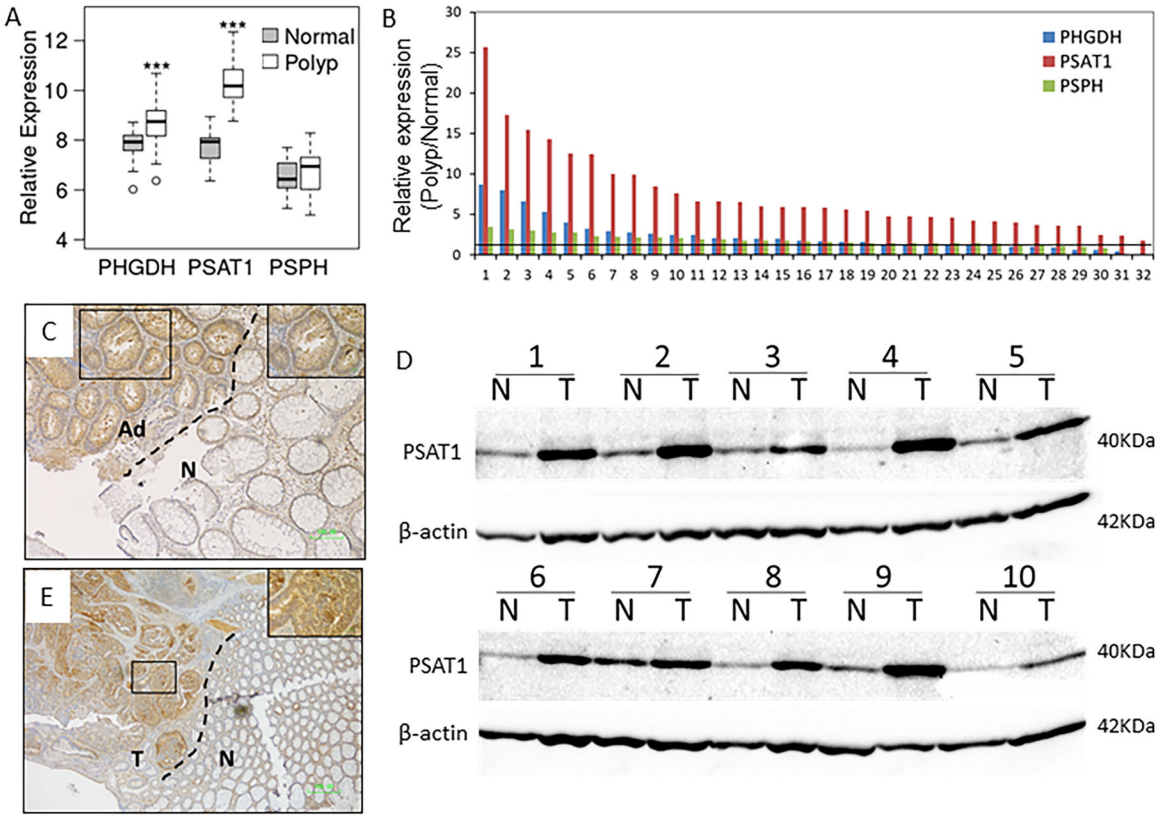

Figure 2.

PSAT1 expression is increased in human colorectal neoplasia. (A) A previously published gene expression profile of 32 pairs of adenoma and normal adjacent colon tissue was mined to determine expression of serine biosynthesis enzymes (34). ***P<0.001 comparing polyp to normal for each gene. (B) The data in A are shown as relative expression of the ratio of adenoma over normal for each gene in each pair of samples. Data are ranked from highest to lowest expression. Black line indicates a value of 1. (C) PSAT1 expression was assessed by immunohistochemistry in tissue sections of colon adenomas (Ad) with normal adjacent tissue (N) (40X) (Inset 200X). (D) Paired colorectal normal and adenocarcinoma samples were probed for PSAT1 expression by western blot. β-actin was used as a loading control. (E) PSAT1 expression was assessed by immunohistochemistry in tissue sections of colon adenocarcinomas (T) with normal adjacent tissue (N) (40X) (Inset 200X).

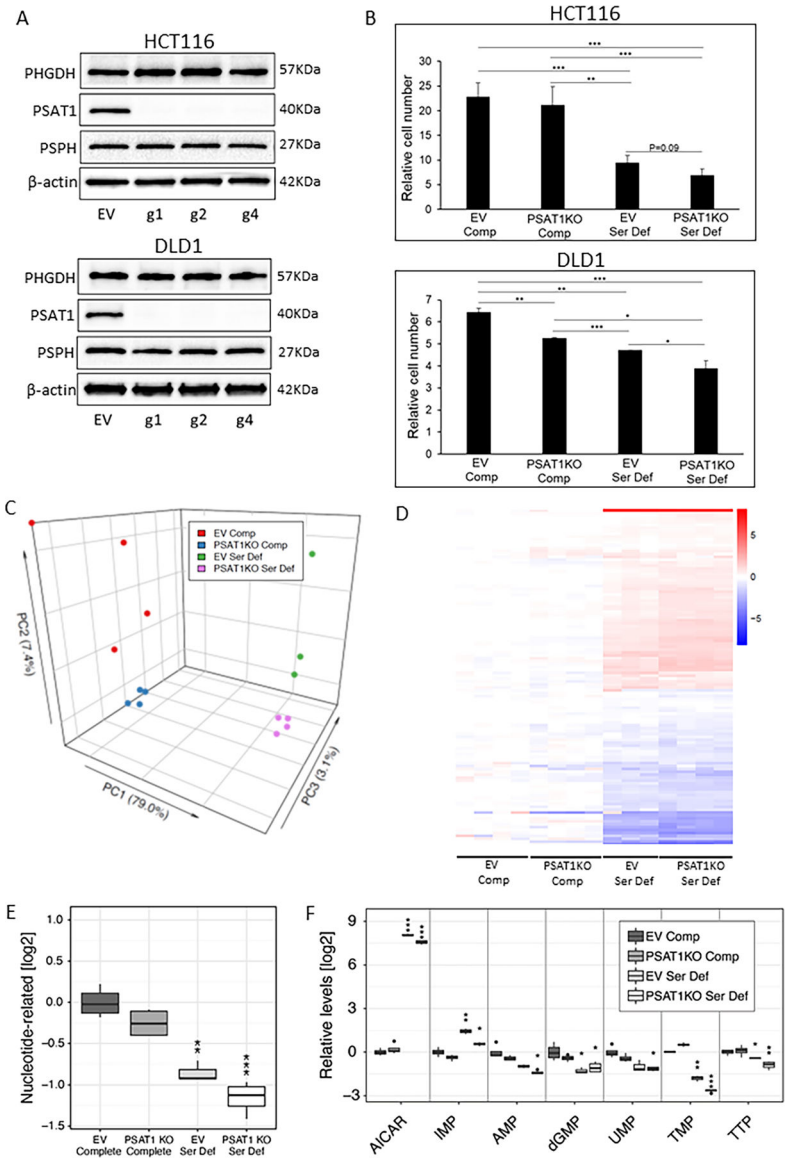

Figure 3.

Restriction of exogenous and endogenous sources of serine maximally suppresses colon cancer cell proliferation and alters metabolism. (A) Western blotting of PHGDH, PSAT1 and PSPH following CRISPR-based deletion of PSAT1 in HCT116 and DLD1 human colon cancer cells containing Cas9, using 3 different guide RNAs. EV = empty vector. (B) Cell number was quantified by flow cytometry-based counting following 4 days of culture and calculated as relative cell number compared to day 0 in HCT116 and DLD1 EV and PSAT1KO cells (containing g4) cultured in Complete (Comp) or Serine Deficient (Ser Def) media. n=3 samples per group. Data represent the means ± S.D. *P<0.05; **P<0.01; ***P<0.001 as indicated. (C-F) EV and PSAT1KO HCT116 cells were cultured in Comp or Ser Def media for 12 hr and the abundance of intracellular metabolites was determined. (C) Principal component analysis of metabolic changes across all samples are shown. (D) Metabolites that were significantly changed after multiple testing correction (FDR<0.05) in

either PSAT1KO Comp, EV Ser Def or PSAT1KO Ser Def HCT116 cells compared to EV Comp cells are shown as a heat map. Scale = log_2 fold change compared to EV Comp group. (E) Results of aggregation-based analysis of metabolite profiling showing the direction of change in the nucleotide category. Data represent log_2 fold change compared to EV Comp cells. **P<0.01; ***P<0.001. (F) log_2 fold change of significantly altered metabolites in the nucleotide category compared to EV Comp cells are shown. *FDR<0.05; **FDR<0.01; ***FDR<0.001. n=3–4 samples per group. AICAR=5-Aminoimidazole-4-carboxamide riboside; IMP=Inosine monophosphate; AMP=Adenosine monophosphate; dGMP=2'-deoxyguanosine 5'-monophosphate; UMP=Uridine 5'-monophosphate; TMP=Thymidine monophosphate; TTP=Thymidine 5-triphosphate.

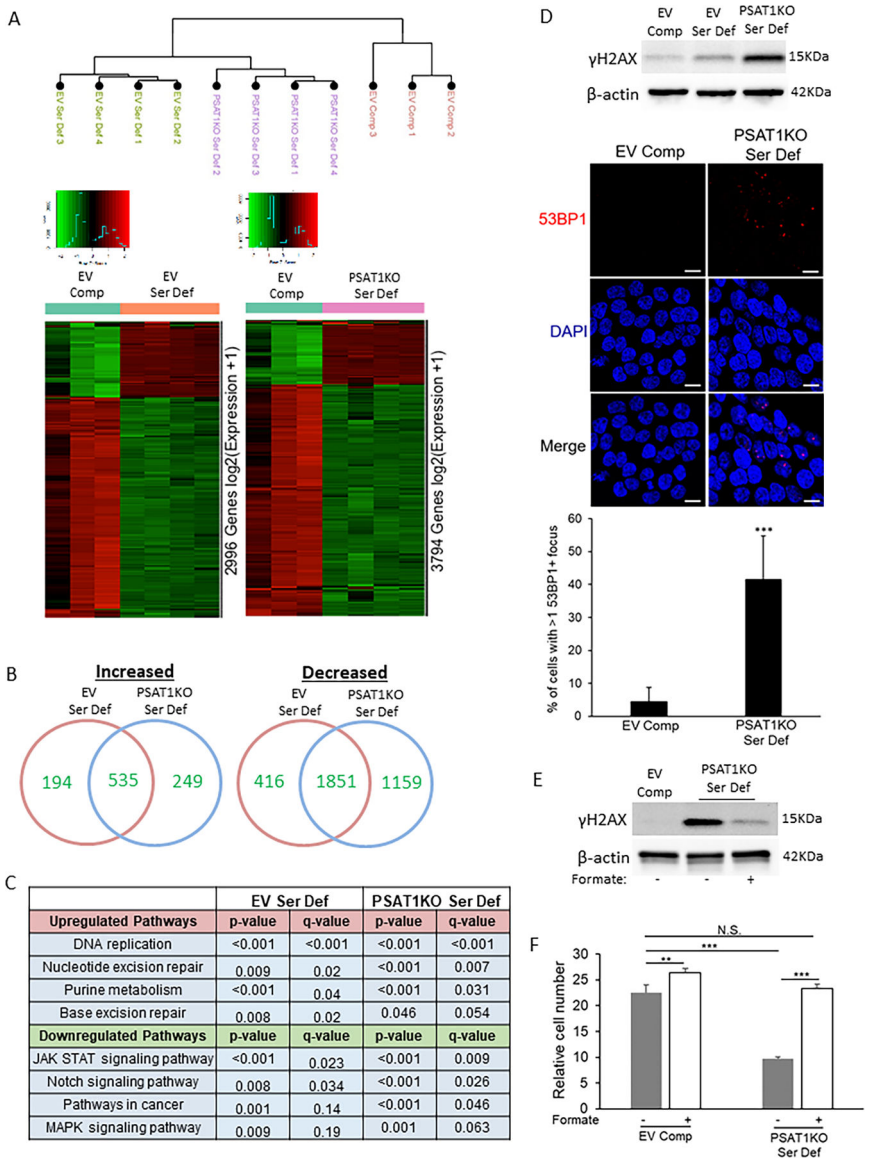

	EV Ser Def		PSAT1KO Ser Def	
Upregulated Pathways	**p-value**	**q-value**	**p-value**	**q-value**
DNA replication	<0.001	<0.001	<0.001	<0.001
Nucleotide excision repair	0.009	0.02	<0.001	0.007
Purine metabolism	<0.001	0.04	<0.001	0.031
Base excision repair	0.008	0.02	0.046	0.054
Downregulated Pathways	**p-value**	**q-value**	**p-value**	**q-value**
JAK STAT signaling pathway	<0.001	0.023	<0.001	0.009
Notch signaling pathway	0.008	0.034	<0.001	0.026
Pathways in cancer	0.001	0.14	<0.001	0.046
MAPK signaling pathway	0.009	0.19	0.001	0.063

Figure 4.

Exogenous and endogenous serine deprivation enhances gene expression changes and DNA damage response compared to exogenous serine restriction alone. (A–C) Empty vector (EV) and PSAT1KO HCT116 cells were cultured in Serine Deficient (Ser Def) medium for 24 hr and global gene expression patterns were evaluated by RNA-seq and compared to EV cells grown in Complete (Comp) medium. (A) Unsupervised hierarchical clustering of experimental groups (top) and those genes with significantly changed expression patterns in EV Ser Def and PSAT1KO Ser Def groups compared to EV Comp cells are shown as a heat map (bottom). (B) Increased or decreased gene expression changes that were shared or unique between the EV Ser Def and PSAT1KO Ser Def groups compared to EV Comp cells, are shown as a Venn Diagram. Values indicate the number of gene expression changes. (C) Pathway changes associated with significantly increased or decreased gene expression changes in EV Ser Def and PSAT1KO Ser Def cells compared to EV Comp cells were

determined by GSEA using KEGG pathways. (D) EV HCT116 cells were grown in Comp or Ser Def media and PSAT1KO HCT116 cells were grown in Ser Def medium for 12 hr and probed for γH2AX by western blot (top), EV Comp or PSAT1KO Ser Def cells were stained for 53BP1 expression by immunofluorescence (middle) and the percent of cells with a number of 53BP1 foci greater than the average of the controls was then determined (bottom). Scale bar = 10μM. (E) EV Comp cells were cultured in the absence of exogenous formate and PSAT1KO Ser Def groups were cultured in the presence or absence of 1mM formate for 12 hr and extracted protein was probed for γH2AX by western blot. (F) Cell proliferation was assessed by flow cytometry-based cell counting in EV Comp and PSAT1KO Ser Def groups in the presence or absence of exogenous formate over a 4 day period and calculated as relative cell number compared to day 0. n=3 samples per group. Data represent the means ± S.D. **P<0.01, ***P<0.001, N.S = not significant

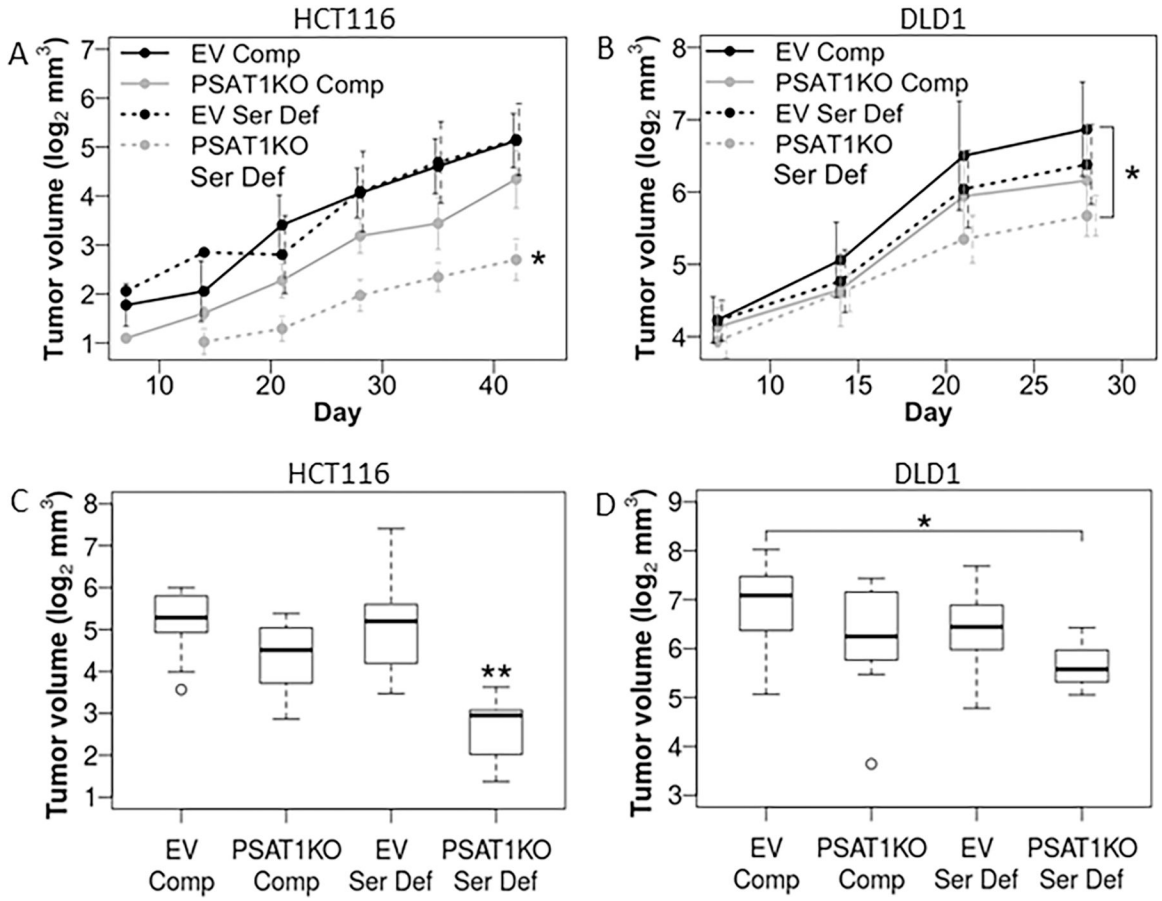

Figure 5.

Combination of *PSAT1* deletion and removal of serine from diet suppresses the growth of colon tumor xenografts. (A–B) Empty vector (EV) and PSAT1KO HCT116 (A) and DLD1 (B) cells were injected into the flanks of nude mice given complete amino acid based diet or Serine Deficient (Ser Def) diet and tumor volume was measured over time. *P<0.05 compared to the other 3 conditions (A) or as indicated (B). n=9–10 tumors per condition. (C–D) Tumor volume data at the terminal time point from panels A and B were evaluated for significant differences among the groups in HCT116 (C) and DLD1 (D) xenografts. **P<0.01 compared to the other 3 conditions (C); *P<0.05 as indicated (D).

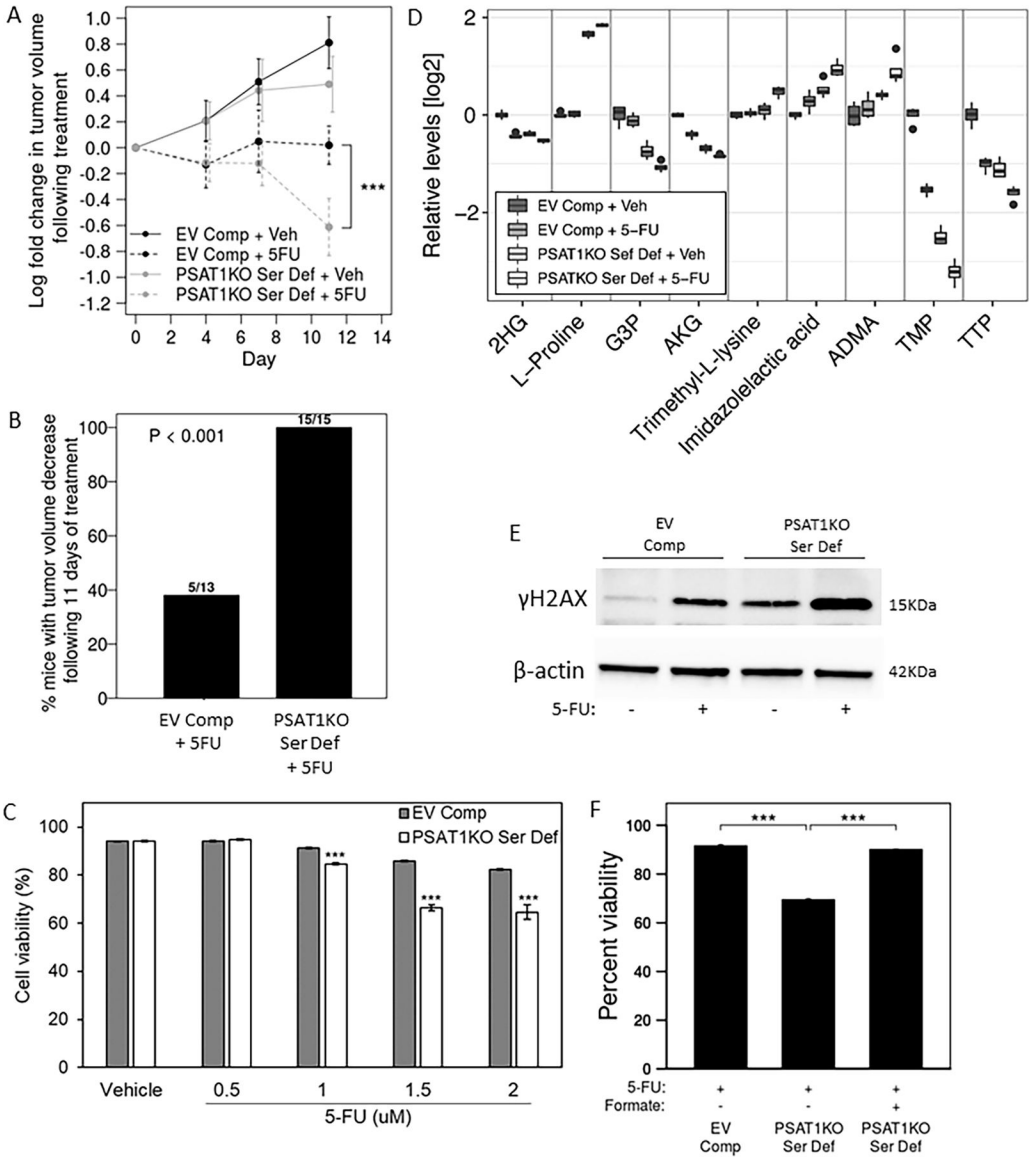

Figure 6.

The anti-tumor activity of 5-FU is augmented when endogenous and exogenous serine are limited. (A–B) Empty vector (EV) and PSAT1KO HCT116 cells were injected into the flanks of nude mice and tumors were allowed to develop over 20 days while mice were fed Complete (Comp) diet. Mice bearing EV tumors were then continued on Comp diet and treated with either 75mg/kg 5-FU or vehicle and mice bearing PSAT1KO tumors were given Serine Deficient diet (Ser Def) and either 5-FU or vehicle every 3–4 days over 11 days. n=13–15 mice per group. (A) Log fold change in tumor volume over time was calculated for each group compared to the start of diet/drug treatment. ***P<0.001. (B) The percent of mice in which a reduction in tumor size occurred following 5-FU treatment, was calculated. (C) EV and PSAT1KO HCT116 cells were grown in Comp or Ser Def media, respectively and treated with either vehicle or 5-FU at 0.5, 1, 1.5 or 2μM for 4 days and viability was assessed by flow cytometry. n=3 samples per group. Data represent the means ± S.D.

***P<0.001 comparing the magnitude of effect of 5-FU treatment in EV Comp *vs.* PSAT1KO Ser Def compared to their respective vehicle-treated groups. (D) Metabolite profiling was carried out in EV Comp or PSAT1KO Ser Def HCT116 cells given vehicle or 1.5 μM 5-FU for 24 hr. Those metabolites that were significantly changed (FDR<0.05) in the PSAT1KO Ser Def cells given 5-FU compared to each of the other 3 conditions and of either the highest or lowest in abundance compared to each of the other three conditions, are shown. n=4 samples per group. Data represent $\log_2$ fold change compared to EV Comp cells treated with vehicle. (E) HCT116 cells were treated under the same conditions as described in panel C but for 12 hr and the expression of γH2AX was evaluated by western blot. (F) EV Comp cells were treated with 1.5 μM 5-FU in the absence of formate and PSAT1KO Ser Def cells were treated with 1.5 μM 5-FU in the presence or absence of formate, and cell viability was examined after 4 days in culture. n=3 samples per group. Data represent the means ± S.D. ***P<0.001. 2HG=2-hydroxyglutarate; G3P=glyceraldehyde 3-phosphate; AKG=alpha-ketoglutarate; ADMA=asymmetric dimethylarginine; TMP=Thymidine monophosphate; TTP=Thymidine 5-triphosphate.